Influence of oxygen flow rates on physical properties of DC reactive magnetron sputtered Zinc Aluminum Oxide thin films

B. RAJESH KUMAR[a,b*], T. SUBBA RAO[b]
[a]*Department of Physics, Sri Venkateswara University, Tirupati-517502, A.P, India*
[b]*Materials Research Lab, Department of Physics, Sri Krishnadevarya University, Anantapur-515003, A.P, India*

Transparent conducting Zinc Aluminum Oxide (ZAO) thin films have been deposited on glass substrates by DC reactive magnetron sputtering technique at oxygen flow rates of 1 sccm - 4 sccm. XRD patterns of ZAO thin films exhibit (0 0 2) preferential orientation with the c-axis perpendicular to the substrate and contains compressive stress. SEM images of ZAO thin films show columnar grains perpendicular to the substrate and some granular grains are also exist in the films. The lowest resistivity of 3.48 x 10^{-4} Ω.cm and a maximum optical transmittance of 90 % are obtained for ZAO film deposited at oxygen flow rate of 3 sccm. The optical direct band gap values of ZAO films increases with the increase of oxygen flow rates.

(Received June 2, 2012; accepted September 20, 2012)

Keywords: ZAO thin films, DC reactive magnetron sputtering, Structural properties, Electrical properties, Transmittance

1. Introduction

Doped ZnO thin films are currently under intense investigation for the development of optoelectronic and energy conversion applications. Minami et al [1] first reported that the resistivity stability at high temperatures can be successfully improved in transparent conducting ZnO films doped with a donor impurity such as Al or Ga. Al-doped ZnO (AZO) is a promising transparent conductive oxide (TCO) considered as a candidate to replace the indium tin oxide. Al doping can dramatically increase the free charge carrier concentration and simultaneously keep the transparency in the visible range. Both these are necessary for the transparent conduction [2, 3]. In particular transparent and conductive Al:ZnO (AZO) films are being considered for manufacturing transparent electrodes in flat panel displays, solar cells and organic light emitting diodes due to their high electro-optical quality, high materials availability and low material cost for large area applications [4-6].

Various deposition techniques have been utilized for Zinc Aluminum Oxide films such as direct current (DC) and radio frequency (RF) magnetron sputtering [7]. Pulsed laser deposition [8], chemical vapor deposition [9], spray hydrolysis [10], and sol-gel [11]. In order to satisfy the demands of good film quality, high-rate and large-area deposition, and low cost of equipment for commercialization of all TCO films, DC magnetron sputtering has been regarded as one of the most attractive and effective fabrication techniques in the mass production of films. In this paper, a systematic study of structural, electrical, and optical properties of ZAO films at different oxygen flow rates has been discussed in detail.

2. Experimental details

Zinc Aluminum Oxide (ZAO) thin films were prepared by DC reactive magnetron sputtering technique. High purity metal targets of Zn (99.999%) and Al (99.99%) with 2 inch diameter and 4 mm thickness are used for deposition on glass substrates. The glass substrates were ultrasonically cleaned in acetone and ethanol, rinsed in an ultrasonic bath in deionized water for 15 min, with subsequent drying in an oven before deposition. The sputter chamber is initially evacuated to a pressure of 10^{-4} Pa and then pure argon gas is introduced into the chamber at a flow rate of 25 sccm (standard cubic centimeters per minute) through mass flow controller (Model GFC 17, Aalborg, Germany). Pure oxygen is let into the chamber through another mass flow controller with varying oxygen flow rates from 1 to 4 sccm. Deposition of the films was carried out at a working pressure of ~ 0.2 Pa after pre-sputtering with argon for 10 min. The distance between the target and substrate is kept at 60 mm and the deposition time is 30 min. Film thickness was measured by Talysurf profilometer. The resulting thickness of all the films is in the range of 300-350 nm. The bias voltage applied for the Zn target is ~ 330-350 V (current, I = 0.30 A) and for Al target is ~220 V (current, I = 0.16 A). XRD (Philips: PW 1830) was used to analyze the crystalline orientation and lattice constant of the ZAO thin films. Surface morphology of the samples has been studied using Hitachi SU 6600 Variable Pressure Field Emission Scanning Electron Microscope (FESEM) with Energy Dispersive Spectroscopy (Horiba, EMAX, 137eV) and AFM (Park XE-100: Atomic Force Microscopy). EDS is carried out for the elemental analysis of prepared thin film samples. The sheet resistance (R_s) of the film was

measured with a four-point probe method. The resistivity of the film (ρ) was calculated using the simple relation $\rho = R_s.d$, where d is the film thickness. The optical transmittance measurements were recorded as a function of wavelength in the range of 300-1200 nm using JASCO Model V-670 UV-VIS-NIR spectrophotometer (Tokyo, Japan).

3. Results and discussion

3.1 Structural properties

XRD patterns of ZAO thin films deposited on glass substrates at different oxygen flow rates are shown in Fig. 1. It is observed that the (0 0 2) diffraction angle shifts from 34° to 33.76° towards lower angles as the oxygen flow rate changes from 1 to 4 sccm. The FWHM increases from 0.18° to 0.40° with increase of oxygen flow rates. An increasing peak width reflects higher amount of micro-stress, the emergence of point defects and smaller grain sizes. In addition, the lattice parameter of c is larger than the ASTM value of 5.20 Å for bulk ZnO and increases as the oxygen flow rate is increased, suggesting that the film contains residual stress along the c-axis and the stress value increases as the oxygen flow rate increases. Similar behavior was previously reported in the literature [12, 13].

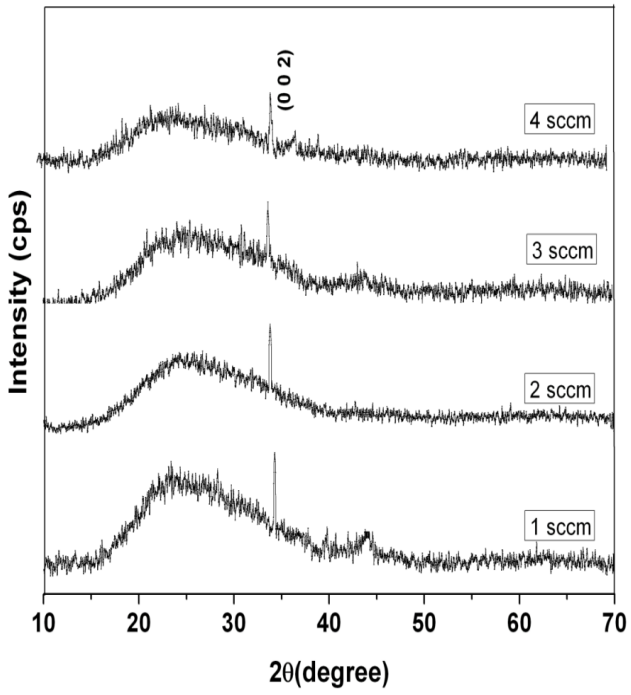

Fig. 1. XRD patterns of ZAO thin films deposited at different oxygen flow rates

The lattice constants and the film stress of ZAO thin films are obtained from XRD data. The lattice constant c can be evaluated by the following formula [14]:

$$\frac{1}{d_{hkl}^2} = \frac{4}{3}\left(\frac{h^2+hk+l^2}{a^2}\right) + \frac{l^2}{c^2} \quad (1)$$

Where a and c are the lattice constants, and d_{hkl} is the crystalline plane distance for indices (h k l). It was found that all d values are larger than that of standard ZnO powder d_o, which is equal to 0.2603 nm. According to equation (1), the lattice constant c is equal to 2d for the (0 0 2) diffraction peak. The lattice constant increases with increase of oxygen flow rate shown in Table 1. Since the radius (0.53Å) of Al^{3+} is smaller than that (0.74 Å) of Zn^{2+}, the increase in the lattice constants is probably due to the incorporation of Al atoms are located at the interstital site rather than Zn site.The crystallite size estimated from Scherrer formula [15] decreased from 41 to 21 nm with the increase of oxygen flow rate from 1 to 4 sccm.

The film stress can be calculated based on the biaxial strain model [16]. The strain in the films in the direction of the c-axis as determined by XRD is $\varepsilon = (c_{film}-c_o)/c_o$, where c_o (=0.5205 nm) is unstrained lattice parameter measured from ZnO powder and c_{film} is the lattice parameter of ZAO film. The films stress σ_{film} parallel to the films surface can be derived by the following formula, which is valid for a hexagonal lattice [17]:

$$\sigma_{film} = \frac{2c_{13}^2 - c_{33}(c_{11}+c_{12})}{2c_{13}} \times \frac{c_{film}-c_o}{c_o} \quad (2)$$

For the elastic constants, data of single-crystalline ZnO have been used c_{11}=208.8, c_{33}=213.8, c_{12}=119.7, c_{13}=104.2 GPa. The following numerical relation for the stress derived from XRD can be obtained:

$$\sigma_{film} = -232.8 \times \varepsilon \ (GPa) \quad (3)$$

From Table 1 it is noticed that the values of stress changed upon changing the oxygen flow rates. An increase of oxygen flow rate led to an increase in the compressive stress. This fact could be attributed to the low substrate temperature used during the deposition. The low mobility would lead to a sub-implantation of the energetic ions into the subsurface. At the same time, the surface atoms could also be knocked deeper into the subsurface of the growing films by the bombardment of energetic ions or atoms. The sub-implanted or knocked atoms in the subsurface could cause high compressive stress levels. As the oxygen flow rate increases the ions would experiment less collisions on the way to the substrate and hence the mobility of the atoms in the films would increase greatly, being able to diffuse from one position to another. Therefore, those atoms trapped in the non-equilibrium position could shift to a more equilibrium position, releasing the strain in the film. This result was in agreement with the ones obtained by other authors in the literature for AZO films deposited on glass substrates [18, 19].

Table 1: Structural parameters of ZAO thin films deposited at various oxygen flow rates

Oxygen flow rate (sccm)	Inter-planar spacing d (nm)	c-lattice constant (nm)	Crystall-ite size D (nm)	Stress σ_{film} (GPa)
1	0.2633	0.5266	41	-2.95
2	0.2648	0.5296	34	-4.30
3	0.2645	0.5290	26	-4.03
4	0.2652	0.5304	21	-4.65

Fig. 2 shows Scanning electron microscopy (SEM) images of ZAO thin films deposited at different oxygen flow rates. All the films grow mainly with columnar grains perpendicular to the substrate and some granular grains are also exist in the films. The films deposited at oxygen flow rate of 2 sccm have the domains formed by aggregation of nanoscale crystallites. The films have an average grain size of 20-45 nm. The compositional elemental data of ZAO films deposited at oxygen flow rate of 3 sccm is shown in Fig. 3.

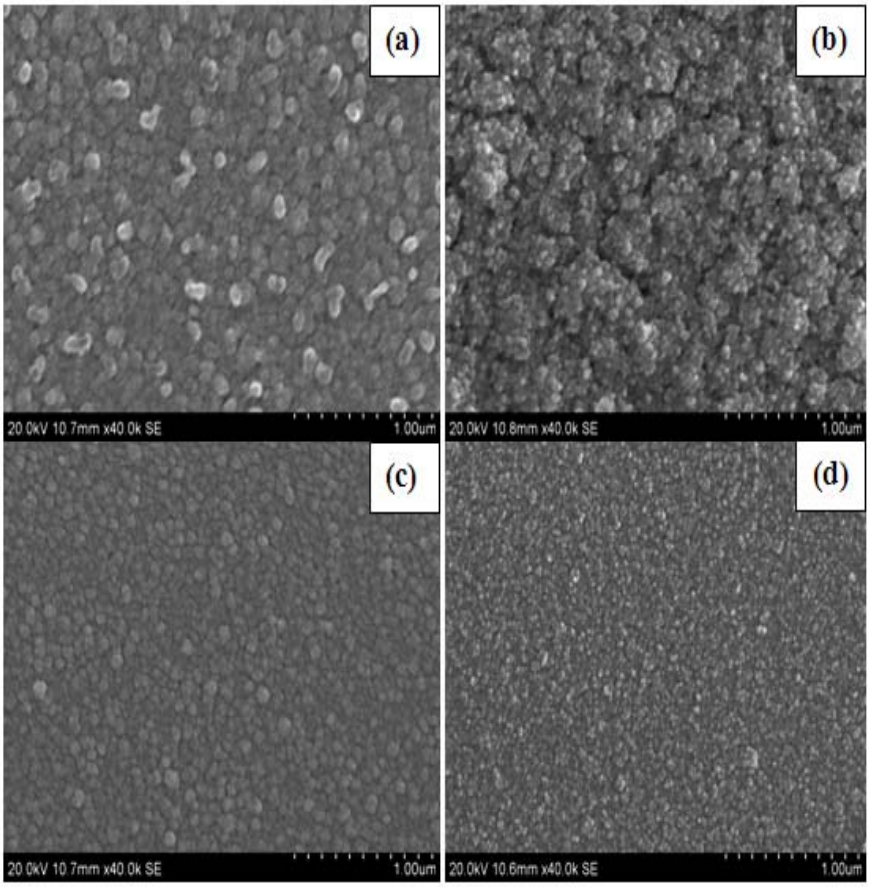

Fig. 2. SEM images of ZAO films deposited at oxygen flow rates of (a) 1 sccm, (b) 2 sccm, (c) 3 sccm and (d) 4 sccm.

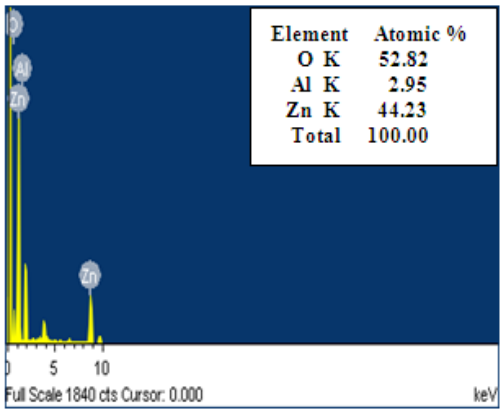

Fig. 3. EDS plot for ZAO film deposited at oxygen flow rate of 3 sccm.

Fig. 4 shows two and three dimensional AFM images of the films deposited at different oxygen flow rates with scanned over an area of 2 μ x 2 μ. AFM images indicate that the increase in the surface roughness by oxygen flow rate was caused by sharp hill-and-valley structure throughout the film surface. But for the film deposited at oxygen flow rate of 2 sccm, the surface is very flat and no very sharp peak appears in the domain. The root mean square (RMS) surface roughness values of ZAO thin films deposited at different oxygen flow rate are shown in Table 2. The maximum RMS surface roughness value is obtained for the film deposited at oxygen flow rate of 2 sccm. For the films grown from a metallic target we observed that films deposited at higher oxygen flow rates had a uniform grain distribution and smaller size. These

observations may be attributed to the introduction of oxygen in the plasma, which could also generate high-energy oxygen neutral atoms. It is generally believed that the formation of grain agglomerates in the film deposited under the introduction of oxygen gas might be due to re-sputtering of high energy neutral oxygen atoms [20]. As oxygen gas content in plasma gas increases, re-sputtering effect by high energy neutral oxygen atoms can increase. Subsequently it might accelerate grain growth or aggregation of particles and thus change the surface topography of the film at the initial stage of the film growth process.

Table 2: RMS surface roughness values of ZAO thin films

Oxygen flow rate (sccm)	RMS surface roughness (nm)
1	1.42
2	2.88
3	1.35
4	1.16

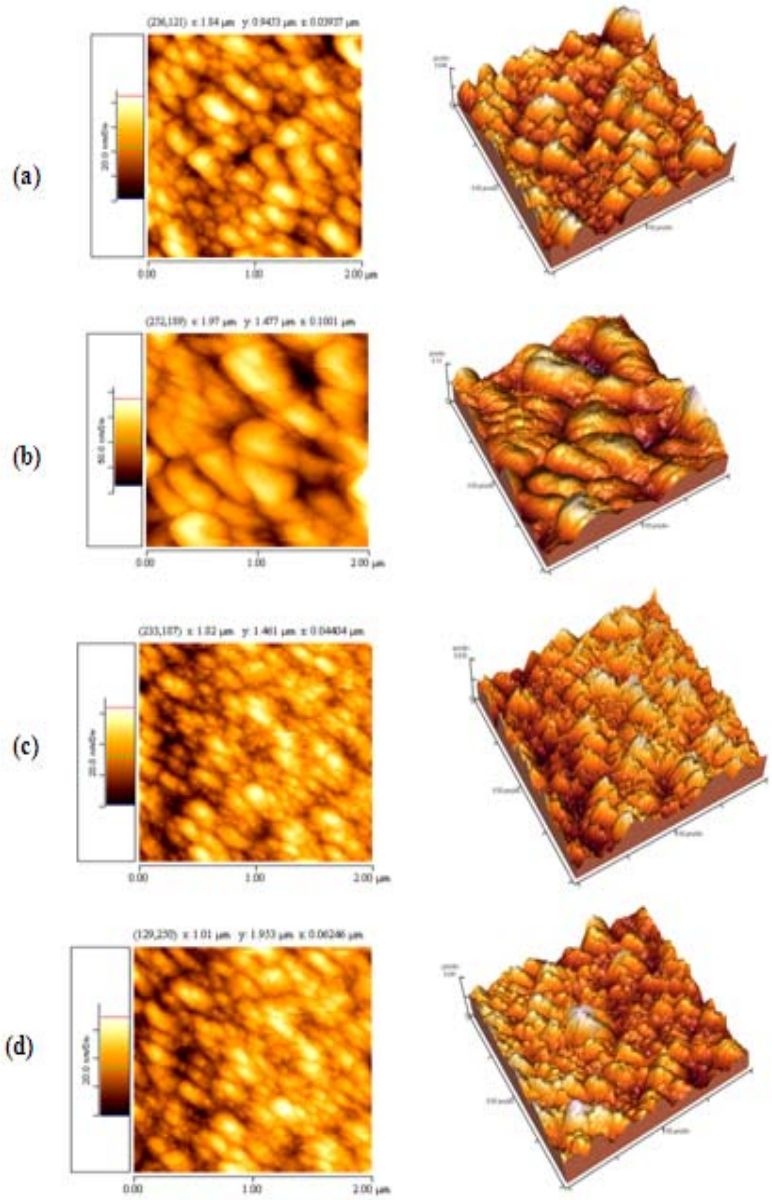

Fig.4 . AFM images of ZAO thin films at oxygen flow rates of (a) 1 sccm, (b) 2 sccm, (c) 3 sccm and (d) 4 sccm.

3.2 Electrical properties

The high conductivity of the films mainly results from a non-stoichiometric composition or doping. Electrons in these films are supplied from donor sites associated with oxygen vacancies of high-valence metal ions. Therefore the oxygen flow rate has a strong influence on the electrical properties of ZAO thin films. The conduction characteristics of ZAO thin films are primarily dominated by electrons degenerated from Al^{3+} ions substitutional sites

of Zn^{2+} ions and Al interstitial atoms. The electrical resistivity of the ZAO films was investigated by four-point probe method at room temperature. The resistivity decreases with the increase of oxygen flow rates shown in Fig. 5. The lowest resistivity of 3.48×10^{-4} Ω.cm is obtained for the oxygen flow rate of 3 sccm.

The sheet resistance value decreases with increase of oxygen flow rate from 1 to 3 sccm and then at 4 sccm it increases (shown in Table 3). The lowest sheet resistance value is obtained for the thin film deposited at oxygen flow rate of 3 sccm.

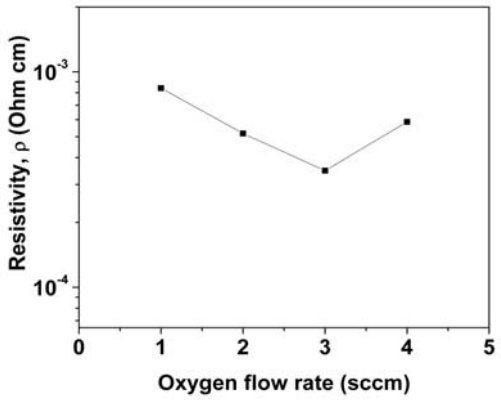

Fig. 5. Electrical resistivity of ZAO films as a function of oxygen flow rates

Mobility of ZAO films at different oxygen flow rates is shown in Fig. 6. The mobility value increases from 11.6 $cm^2V^{-1}sec^{-1}$ to 27.7 $cm^2V^{-1}sec^{-1}$ with the increase of oxygen flow rate from 1 to 3 sccm and then decreased to 24.6 $cm^2V^{-1}sec^{-1}$ for the oxygen flow rate of 4 sccm. The maximum mobility for ZAO films is obtained for ZAO deposited at 3 sccm. The mobility of ZAO thin films with carrier concentration of 10^{19} – 10^{20} cm^{-3} is determined by both the ionized impurity scattering and grain boundary scattering [21]. The increase in mobility is attributed to enhancement of oxygen release and the decrease of grain boundary scattering due to thin film densification and improvement of crystallization.

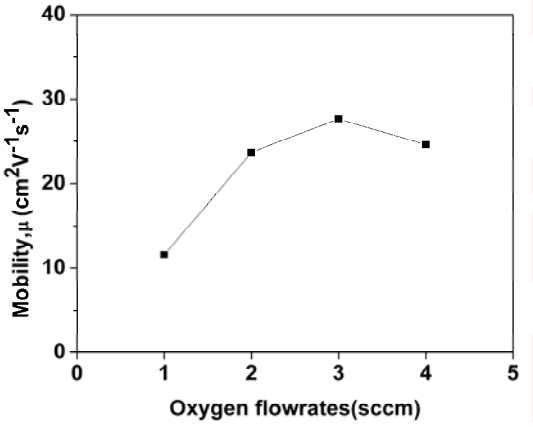

Fig. 6. Variation of mobility of ZAO films at different oxygen flow rates.

3.3 Optical properties

Fig. 7 shows the transmission spectra of ZAO thin films deposited at different oxygen flow rates. An average transmittance in the range of 83 – 90% is obtained for the prepared samples. The absorption edge of all the films is around 352 – 365 nm. The absorption edge slightly shifts to the shorter wavelength as the oxygen flow rate increases. This is mainly attributed to Burstein-Moss effect, since the absorption edge of the degenerate semiconductor is shifted to shorter wavelength with increasing carrier concentration.

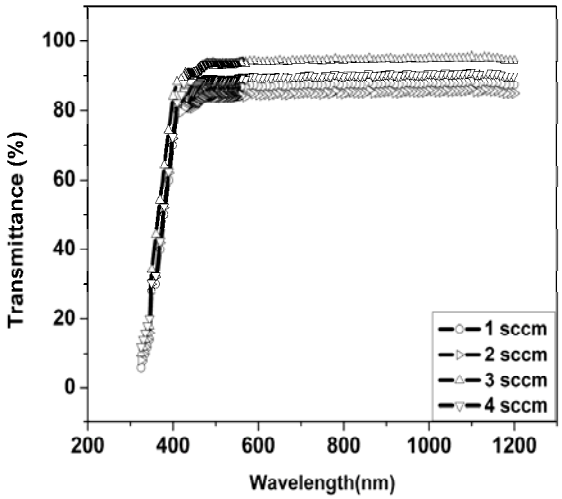

Fig. 7. Transmission spectra of ZAO films deposited at various oxygen flow rates.

The optical band gap, E_g is determined from the dependence of absorption coefficient values (α) on the photon energy, using Tauc's relation [22]

$$(\alpha h\nu) = B(h\nu - E_g)^n \quad (4)$$

where B is a parameter that depends on the transition probability, E_g is the optical band gap energy of the material, hν is the photon energy and n is an index that characterizes the optical absorption process and is theoretically equal to 2 and ½ for indirect and direct allowed transitions respectively.

Fig. 8 shows the plot of $(\alpha h\nu)^2$ versus photon energy hν. The optical band gap energy (E_g) of the films was obtained by extrapolating the linear absorption edge part. The optical band gap increases with increase of oxygen flow rate. The optical band gap values are shown in Table 3. The broadening effect of optical band width can be understood based on the Burstein-Moss effect with a consideration of the free electrons to be damped primarily by ionized impurity scattering [23]. The Fermi energy level shifts to the higher energy side. The increase of carrier concentration confirms the situation.

Table 3: Electrical sheet resistance and optical band gap values of ZAO films.

Oxygen flow rate (sccm)	Sheet resistance (Ω/sq)	Optical band gap (eV)
1	23.2	3.41
2	14.8	3.45
3	10	3.48
4	16.7	3.53

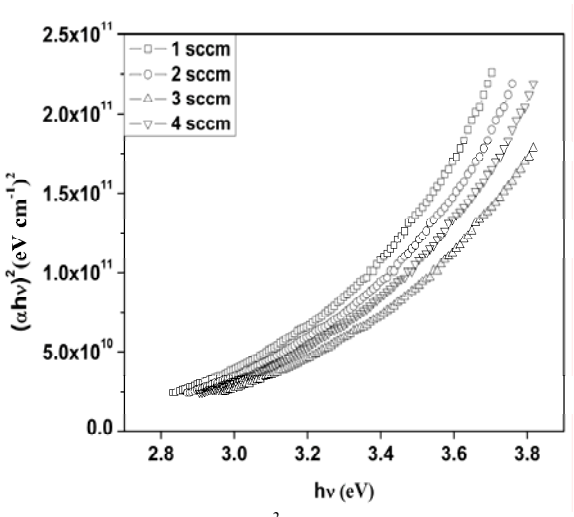

Fig. 8. Variation of $(\alpha h\nu)^2$ versus photon energy hν of ZAO thin films deposited at different oxygen flow rates.

The energy band gap widening ΔE_g is related to carrier concentration though the following equation [24]

$$\Delta E_g = \left(\frac{h^2}{8m^*}\right)\left(\frac{3N}{\pi}\right)^{\frac{2}{3}} \quad (5)$$

where h is the Planks constant, m* is the electron effective mass in conduction band, and n is the carrier concentration. The carrier concentration of ZAO thin films are determined from equation (5) and is found to be in the range of 3.08×10^{20} cm^{-3} – 9.30×10^{20} cm^{-3}. The maximum carrier concentration is obtained for the ZAO film deposited at oxygen flow rate of 3 sccm.

4. Conclusion

ZAO thin films have been grown by DC reactive magnetron sputtering technique on glass substrates by varying oxygen flow rates from 1 to 4 sccm. The deposited ZAO films have a preferred crystalline orientation of (0 0 2) direction. The experimental results show that the minimum resistivity of 3.48×10^{-4} Ω.cm and a maximum optical transmittance of 90% are obtained for the oxygen flow rate of 3 sccm. The low resistivity of ZAO resulted mainly from stoichiometric variation. The conduction characteristics of ZAO films are dominated by O^{2-} vacancies, Zn interstitial atoms, Al ions on substitutional site of Zn ions and Al interstitial atoms. This indicates that these films satisfy basic requirement for the TCO films for display and solar cell applications.

Acknowledgements

The authors are thankful to UGC, New Delhi, India for financial support under the major research project (F.NO.37-346/2009, SR).

References

[1] T. Minami, H. Sato, H. Nanto, S. Takata, Jpn. Appl.Phys. **24**, L781 (1985).
[2] S. Takata, T. Minami, H. Nanto, Thin Solid Films **135**,183 (1986).
[3] Jiaheng Wang, Lei Meng, Yang Qi, Maolin Li, Guimei Shi, Meilin Liu, J. Cryst. Growth, **311,** 2305 (2009).
[4] X.T. Hao, F.R. Zhu, K.S.Ong, L.W.Tan, Semicond. Sci.Technol. **21**, 48 **(**2006).
[5] C.G.Granqvist, Sol. Energy Mater.Sol.Cells, **91**, 1529 (2007).
[6] T.Minami, Thin Solid Films **516**, 5822 (2008).
[7] C. Agashe, O. Kluth, G. Schope, H. Siekmann, J. Hupkes, B.Rech, Thin Solid Films **442**,167 (2003).
[8] H. Agura, A. Suzuki, T. Matushita, T. Aoki, M. Okuda, Thin Solid Films, **445**, 263 (2003).
[9] H. Sato, T. Minami, S. Takata, T. Miyata, M. Ishii, Thin Solid Films, **236**, 14 (1993).
[10] P.Nunes, E.Fortunato, R.Martins, Thin Solid Films**, 383**, 277 (2001).
[11] A.E.Jimenez-Gonzalez, J.A.S.Urueta, R.Suarez-Parra, J.Cryst.Growth, **192**, 430 (1998).
[12] M. Chen, Z. L. Pei, X. Wang, C. Sun, L. S. Wen, Mat**.** Lett**. 48**, 137 (2001).
[13] L. J. Meng, M.P.Santos, Vacuum, **46**, 6090 (1995).
[14] G. J. Fang, D .J Li, B. L. Yao, Phys.Stat.Sol. A, **93**, 139 (2002).
[15] B.D.Cullity, Editor, Elements of X-ray diffraction, Addition-Wesley, London (1959).
[16] A.Segmuller, M.Murakami, R.Roscoberg, Editor, Analytical Techniques for Thin Films, Academic Press, Boston (1988).
[17] R.Cebulla, R.Wendt, K.Ellmer, J.Appl.Phys. **83**, 1087 (1998).
[18] W.Li, Y.Sun, Y.Wnag, H.Cai, F.Liu, Q.He, Sol. Energy Mater. Sol.Cells, **91**, 659 (2007).
[19] R.J.Drese, M.Wuttig, J.Appl.Phys. **98**, 073514 (2005).
[20] S.Mishra, C.Ghanshyama, N.Rama, R.P.Bajpai, R.K.Bedi, Sens. Actuators, B **97**, 387 (2004).
[21] T.Minami, S.Suzuki, T.Miyata, Thin Solid Films, **53**, 398 (2001).
[22] J. Tauc, R. Grigorovici, A. Vancu, Phys. Stat. Sol. **15**, 627 (1966).
[23] Z.C.Jin, U, I. Hamberg, C.G.Granqvist, J. Appl. Phys. **64**, 5117 (1988).
[24] F.Urbach, Phys.Rev. **92**, 1324 (1953).

*Corresponding author: rajphyind@gmail.com